



Lead-induced changes of cytoskeletal protein is involved in the pathological basis in mice brain

Yaming Ge¹ · Lingli Chen^{1,2} · Xianghe Sun³ · Zhihong Yin¹ · Xiaochao Song¹ · Chong Li¹ · Junwei Liu¹ · Zhixing An¹ · Xuefeng Yang¹ · Hongmei Ning¹

Received: 16 October 2017 / Accepted: 18 January 2018 / Published online: 13 February 2018
© Springer-Verlag GmbH Germany, part of Springer Nature 2018

Abstract

Lead poisoning is a geochemical disease. On the other hand, lead is highly carcinogenic and exhibits liver and kidney toxicity. This element can also cross the blood-brain barrier, reduce learning and memory ability and damage the structure of the cerebral cortex and hippocampus. To further investigate the mechanism of lead neurotoxicity, 4-week-old Kunming mice were used to explore the effects of different concentrations of Pb²⁺ (0, 2.4, 4.8 and 9.6 mM) for 9 days. In this study, pathological and ultrastructural changes in brain cells of the treated group were related to damages to mitochondria, chromatin and the nucleus. Lead content in blood was tested by atomic absorption spectroscopy, which showed high lead concentrations in the blood with increasing doses of lead. Distribution of lead in nerve cells was analysed by transmission electron microscopy with energy dispersive spectroscopy. Data showed the presence of lead in nucleopores, chromatin and nuclear membrane of nerve cells in the treatment groups, whereas lead content increased with increasing doses of lead acetate. Finally, microtubule-associated protein 2 (MAP2) mRNA and protein expression levels were detected by real-time PCR and Western blotting, which showed a reduction in MAP2 expression with increasing lead doses in the mouse brain. These findings suggest that acute lead poisoning can cause significant dose-dependent toxic effects on mouse brain function and can contribute to better understanding of lead-induced toxicity.

Keywords Lead poisoning · Mice · Neurons · Morphology · MAP2

Introduction

Lead (Pb) is a well-recognised environmental pollutant and poses a serious health concern to humans and animals (Bansod et al. 2017; Shenai-Tirodkar et al. 2017). This element can be found in soil, water and the atmosphere (Rosen et al. 2017); lead contamination will be permanently present in the environment (Kazemeini et al. 2013). Lead is toxic to

plants and animals, not only affecting normal plant growth but also threatening the health of humans and animals through its enrichment in the food chain (Flora et al. 2012). Dietary Pb intake is the primary cause of human and animal exposure to this metal (Nascimento et al. 2016; Farzin et al. 2008; Caldas et al. 2016). Leasure et al. (2008) confirmed that gestational lead exposure produced permanent male-specific defects. Lead exposure caused seminiferous epithelium transformation in all stages of spermatogenesis, with outcomes including markedly smaller size of sperms, loss of normal spermatogenic cell organisation and disorganisation of basement membrane with vacuolisation (Anjum et al. 2016). Some studies have shown that Pb exposure is associated with DNA damage and causes a decrease in DNA repair capacity, indicating a potential health concern for Pb-exposed populations (Jannuzzi and Alpertunga 2016; Sohail et al. 2017). Pb was also shown to alter DNA methylation in Wister rats (Sun et al. 2017). Pb treatment significantly decreased the activity of mitochondrial complexes and increased the expression of apoptosis-related genes (Jin et al. 2017).

Yaming Ge and Lingli Chen have equal contribution.

Responsible editor: Philippe Garrigues

✉ Hongmei Ning
pangpangning@126.com

¹ College of Animal Science and Veterinary Medicine, Henan Institute of Science and Technology, Xinxiang 453003, China

² Shanxi Agriculture University, Taigu 030801, China

³ Nanle Buteau of Agriculture and Animal Husbandry, Puyang 457400, China

Various researches have raised people's awareness on the dangers of Pb pollution and the harmful effects of Pb on the central nervous system (Verstraeten et al. 2008; Wagner et al. 2017). Microtubule-associated proteins (MAPs) specifically combine with microtubules, which constitute approximately 10 to 15% of the microtubule structure, and are in a constant state of dynamic instability both in vivo and in vitro. MAP2 acts as the most abundant mammalian brain protein that is specifically expressed in neurons (Suzuki et al. 2011; Kubatiev and Pal'tsyn 2012). MAP2 is a prominent regulator of microtubule assembly and dynamic stability, both of which play significant roles in brain development (Chen et al. 2015). MAP2 belongs to the MAP family, and it plays an important role in plasticity and stability of nerve cell axons and dendrites (Gumy et al. 2017). Zhang et al. observed that the damages of Pb to cerebral ganglia cells include cell apoptosis, lysosome proliferation, cytoskeletal disruption and oxidative stress in the cerebral ganglion (Zhang et al. 2016). The projection domains of MAP2 and Tau are involved in regulation of microtubule spacing within neurons (Chen et al. 1992). Hyperphosphorylation of Tau is involved in the pathogenesis of neurological disorders; Pb up-regulates Tau protein levels and induces Tau hyperphosphorylation in the rat brain cortex and cerebellum, possibly leading to impairment of cytoskeleton stability and neuronal dysfunction (Gaśowska et al. 2016).

To determine the effects of acute Pb poisoning on mice, morphological changes in mouse brains were examined, and the role of MAP2 in the mouse brain after Pb poisoning was explored. The information gained will provide theoretical basis for further studies of the mechanism of injury resulting from lead poisoning.

Materials and methods

Animals

This study used healthy Kunming mice, which were provided by the Animal Center of Xinxiang Medical University (Xinxiang, China). All mice were maintained at relative humidity of 42–57% and at room temperature (24 ± 2 °C), with unlimited access to water and food under a 12-h light/12-h dark cycle. Four-week-old female ($n = 20$) and male ($n = 20$) mice were used for the experiments. The mice were randomly separated into four groups (5 female and 5 male mice per group). Each group was provided with water with different lead concentrations: control group (distilled water), low lead concentration group (Pb^{2+} , 2.4 mM), moderate lead concentration group (Pb^{2+} , 4.8 mM) and high lead concentration group (Pb^{2+} , 9.6 mM). Nine days after Pb acetate treatment, mice were fasted for 24 h, and anticoagulant blood and brain samples were collected for analysis. All experiments using

mice were approved and performed according to the guidelines of the Institutional Ethics Committee on Experimental Animals.

Determination of blood Pb concentration

After weighing, we enucleated the eyeballs of mice for whole-blood collection. Values provided (mg/L) represent the mean \pm SEM for 5 male and 5 female mice per treatment. Samples were analysed by atomic absorption spectroscopy (AAS) according to the method of de Oliveira et al. (2017).

Histopathological assessment

For histopathological studies, the brains of treated and untreated animals were kept in 10% formalin in separate glass vials for fixation by immersion for 24 h. Samples were washed with running water for 6–7 h and subsequently dehydrated in a graded alcohol series. Fixed and dried tissues were rinsed with xylene twice for 15 min. Paraffin-embedded tissue sections were cut to a thickness of 5 μm and stained with haematoxylin and eosin for histological examination to assess brain damage. Histopathological changes in brain tissues were observed under a standard optical microscope.

Transmission electron microscopy (TEM)

Mouse brain tissues were fixed with 2.5% glutaraldehyde. After washing thrice with PBS, the tissues were post-fixed in 1% osmium tetroxide followed by 50% ethanol for 15 min, 70% ethanol for 15 min, 95% ethanol for 15 min, thrice in 100% ethanol for 15 min and twice in 100% propylene oxide for 15 min. Embedding of fixed tissues was started in 1:1 propylene:resin for 1–2 h, followed by 2:1 propylene:resin for 1–2 h and pure resin overnight. Slices were obtained to observe ultrastructural changes, and scanning and photography were performed using TEM with energy dispersive spectroscopy (TEM-EDS).

Real-time PCR

Total RNA was extracted from mouse brains with Trizol reagent (Life Technology). Total RNA concentration was measured using a Nanodrop spectrophotometer (Thermo Scientific, Waltham, MA). First-strand cDNA was synthesised from 1 μg of total RNA using the M-MLV reverse transcriptase (Takara, Dalian, China). RT-PCR was performed using a Quantstudio 5 real-time system (Thermo Fisher Scientific, Waltham, MA) with SYBR Green PCR Kit (Qiagen, German). Relative expression of the target gene was normalised to GAPDH, and primer sequences are shown in Table 1.

Table 1 Primer sequences with their corresponding PCR product sizes

Gene	Accession no.	Primer sequences (5'-3')	Size of productions (bp)
MAP2	M21041	Forward: CAGCAGAGGTCCCAAGTGAG Reverse: GAAACAAGCAGGTCGGAGAT	103
GAPDH	GU214026	Forward: CCTTCCGTGTTCTACCC Reverse: GCCCTCAGATGCCTGCT	194

Western blotting

Mouse brain tissues (< 100 mg) were lysed with ice-cold RIPA protein lysis buffer for 30 min, and the supernatant was then collected after centrifugation at 12,000×g for 10 min at 4 °C. Protein concentrations were determined with a Bradford assay kit (Bio-Rad). Protein samples mixed with SDS loading buffer were boiled for 10 min and separated with 10% SDS–polyacrylamide gel electrophoresis. After separation, the proteins were transferred to PVDF membranes and blocked in 5% non-fat milk for 2 h at room temperature. The membranes were incubated with MAP2 rabbit monoclonal antibody (CST, German, #8707) at 4 °C overnight. After incubation with HRP-conjugated goat antirabbit IgG antibody for 1.5 h at room temperature, ECL reagent (Thermo Fisher Scientific, Waltham, MA) was used to visualise the reactive bands, which were exposed to radiography films. The resulting protein bands were analysed using Image J software (National Institutes of Health, USA).

Statistical analysis

Statistical analyses consisted of mean ± SEM and paired-sample *t* tests using SPSS statistics software version 17.0 (IBM Corp, Armonk, NY, USA). *P* < 0.05 and *P* < 0.01 were considered significant.

Results

Morphology of brain tissues after lead exposure

Compared with the controls, results of morphological evaluation by light microscopy showed no remarkable difference in the number of glial and pyramidal cells in mouse brain in the 2.4-mM group. However, in the 4.8- and 9.6-mM groups, the shapes of pyramidal cells changed from irregular to elliptical, whereas the number of heterochromatin reduced in pale nuclei. Numerous nuclei have also shrunken and presented thickened membranes (Fig. 1c, d). Ultrastructural changes in nerve cells were determined by TEM. In the control group, abundant organelles were observed in the cytoplasm, the nuclear membrane and mitochondrial cristae can be observed and ribosomes were uniformly distributed in the cytoplasm (Fig. 2a). No distinct ultrastructural changes were observed in cortex

neurons in the 2.4-mM group (Fig. 2b). However, in the 4.8-mM group, results showed no evident nuclear membrane changes, degranulation of endoplasmic reticulum, swelling of mitochondria nor polymerisation of ribosomes (Fig. 2c). The most notable changes were observed in the 9.6-mM group, which exhibited dissolution and thickening of the nuclear membrane, fusion or disappearance of mitochondria, disintegration of endoplasmic reticulum and increased number of secondary lysosomes (Fig. 2d). These data suggest that lead acetate affected the morphology of mouse brain tissues and ultrastructure of nerve cells.

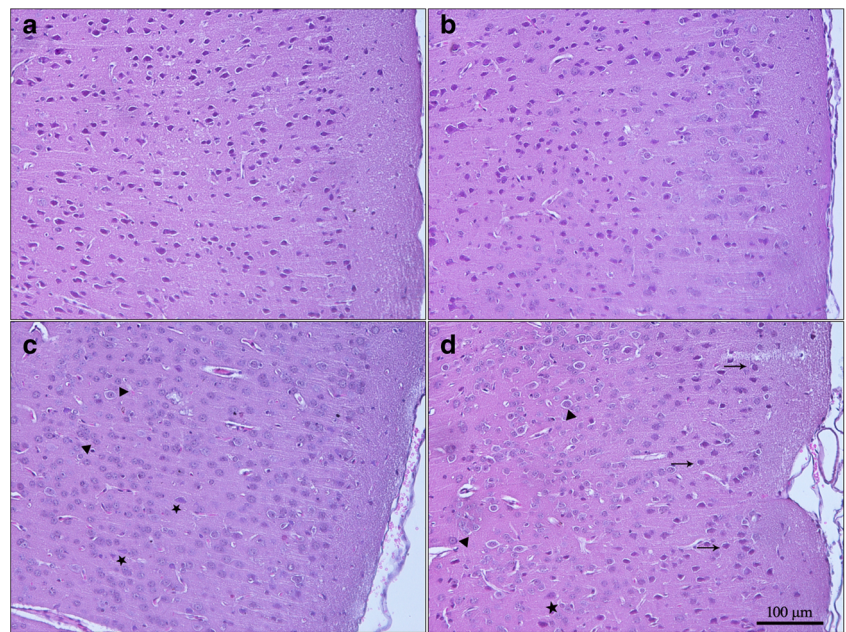
Lead concentration in blood

As shown in Fig. 3, compared with the control group, lead concentrations of anticoagulated blood in the treatment groups increased significantly by 29.69, 31.75 and 33.74 times with increasing doses (*P* < 0.01). However, no significant differences were observed among the treatment groups (*P* > 0.05). Lead can spread throughout the body via the blood and thus injure other organs and systems (Jin et al. 2017; Sun et al. 2017).

Distribution of lead in mouse brain cells

TEM-EDS analysis, with 0.5% sensibility, can be used for semi-quantitative analysis of Pb²⁺ and its distribution in cell nuclei of the brain. Percent weight of Pb²⁺ (wt%), which indicates the proportion of one-point Pb weight in the total amount, is the most significant feature in this analysis. EDS analysis failed to detect the spectral peak of lead in the untreated and 2.4-mM groups. However, spectral peaks can be found in nucleopores, chromatin and nuclear membranes in nerve cells of the 4.8- and 9.6-mM experimental groups (Fig. 4). In the 4.8-mM group, wt% in nucleopore, chromatin and nuclear membrane reached 0.41, 0.59 and 1.85, respectively. On the other hand, in the 9.6-mM group, wt% in nucleopore, chromatin and nuclear membrane totalled 1.48, 1.04 and 0.6, respectively (Table 2). These data indicate that lead can cross the blood-brain barrier to disrupt the brain, and that lead content in nerve cells increased with increasing exposure to lead acetate.

Fig. 1 Histopathological changes of mouse brains exposed to lead acetate. **a** Control, **b** 2.4 mM, **c** 4.8 mM, **d** 9.6 mM, $\times 200$. The arrows imply pyramidal cell change to elliptic, the triangle means nucleolus shrunken, and the five-pointed star is pale nuclei

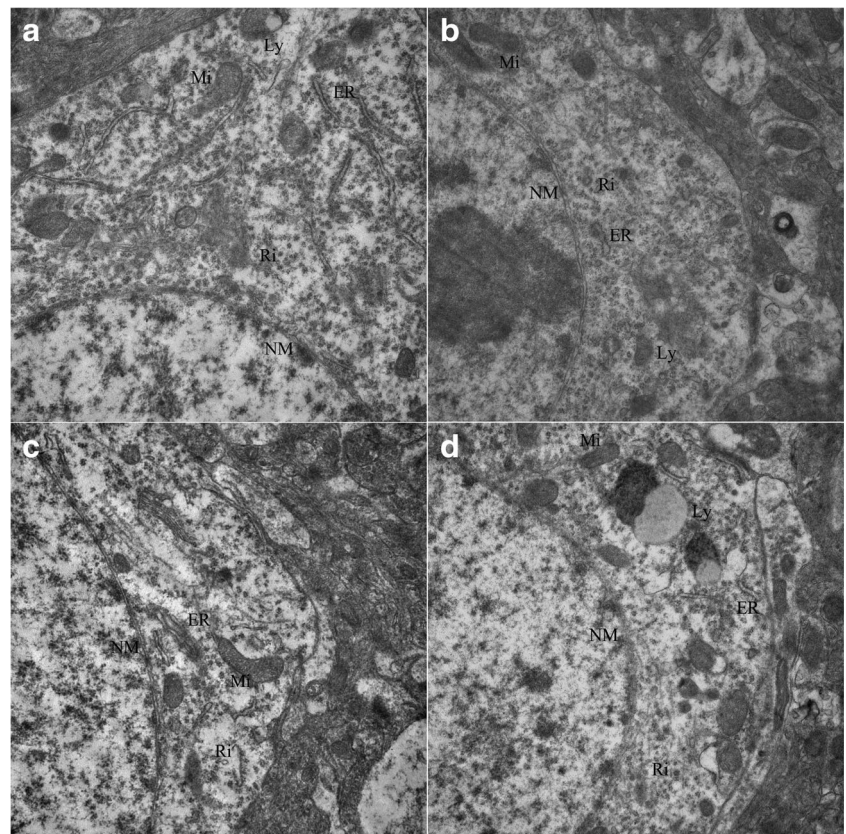


Effect of lead on MAP2 mRNA and protein expression

MAP2 belongs to the structural MAP family, and reduction in MAP2 may cause morphological and functional changes in cells. This study measured the expression of MAP2 in mouse brain tissues by RT-PCR and Western blotting. As shown in

Figs. 5a and, RT-PCR analysis revealed that expression of MAP2 mRNA in the brain tissues of mouse treated with 4.8 or 9.6 mM lead acetate remarkably decreased compared with the controls (65.4 and 72.1%, respectively, $P < 0.05$), but this decrease was not significant in the 2.4-mM group (7%, $P > 0.05$). Western blotting was performed to determine

Fig. 2 Ultrastructure of neurons exposed to lead acetate ($\times 25,000$). **a** Control group, **b** 2.4 mM group, **c** 4.8 mM group, **d** 9.6 mM group. Mi, mitochondrion; NM, nuclear membrane; ER, endoplasmic reticulum; Ri, ribosome; Ly, lysosome



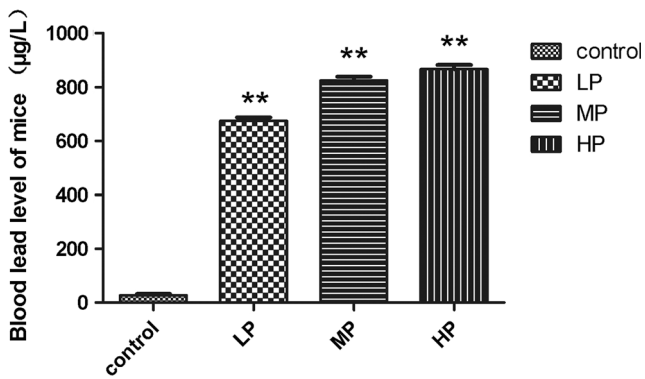


Fig. 3 Blood lead levels of mouse. Control represents untreated mice; LP, low lead group (Pb²⁺, 2.4 mM); MP, moderate lead group (Pb²⁺, 4.8 mM); and HP, high lead group (Pb²⁺, 9.6 mM). **Significantly different from the control (*P* < 0.01)

MAP2 protein levels (see Fig. 5b). Compared with the controls, MAP2 protein levels decreased by 17.6, 24.3 and 40.4%

in the experimental groups (*P* < 0.05), and significant difference was noted in the 9.6-mM group (*P* < 0.01). These data suggest that lead acetate treatment caused the decrease in both mRNA, and protein levels of MAP2 were decreased in mouse brain tissues.

Discussion

Lead is one of the most well-studied metal elements, and its accumulation in organisms can cause harmful effects over time (Flora et al. 2012; Piechnik et al. 2017). Isotopic data have shown that Pb transfers from the maternal skeleton to infants via breast milk (Gulson et al. 2016), and younger organisms accumulate higher amounts of lead compared with adults (Nascimento et al. 2016). Lead is absorbed into the bloodstream via the gastrointestinal tract and can be deposited

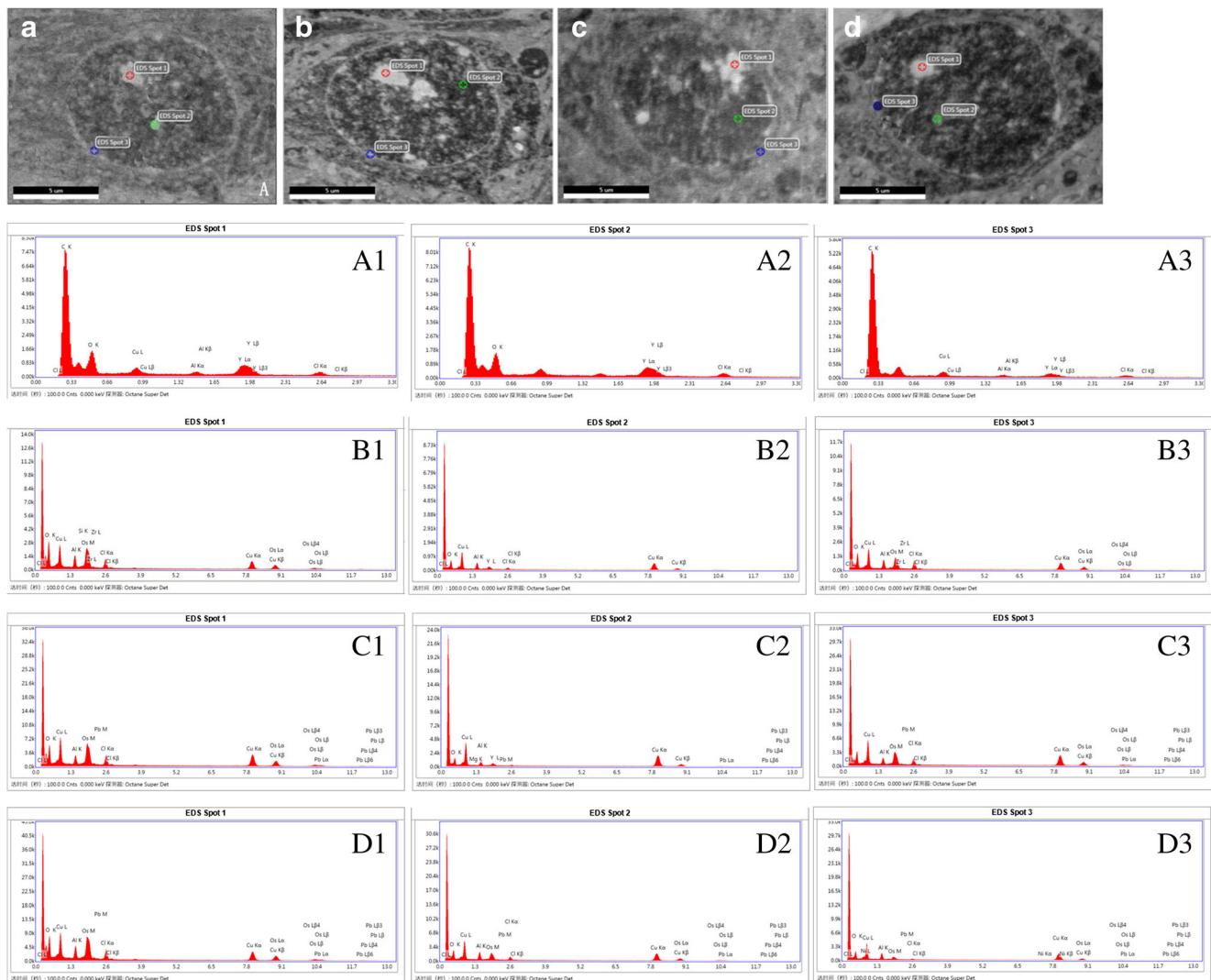


Fig. 4 The distribution of lead in mouse brains. Energy spectrum analysis of mouse brain cells exposed to lead acetate (× 80,000). **a** Control group, **b** 2.4 mM group, **c** 4.8 mM group, **d** 9.6 mM group. A1–A3, three spots

of the control group. B1–B3, three spots of the 2.4 mM group. C1–C3, three spots of the 4.8 mM group. D1–D3, three spots of the 9.6 mM group

Table 2 Lead content analysis of mouse brain cells exposed to lead acetate

Group	Control group			2.4 mM			4.8 mM			9.6 mM		
	1	2	3	1	2	3	1	2	3	1	2	3
Spot	1	2	3	1	2	3	1	2	3	1	2	3
Weight%	0.00	0.00	0.00	0.00	0.00	0.00	0.41	0.59	1.85	1.48	1.04	0.60
Aotm%	0.00	0.00	0.00	0.00	0.00	0.00	0.08	0.10	0.62	0.24	0.17	0.10
Net strength	0.00	0.00	0.00	0.00	0.00	0.00	7.95	4.34	17.39	39.10	10.19	4.43
Error%	0.00	0.00	0.00	0.00	0.00	0.00	37.72	16.10	12.94	9.38	11.88	25.35

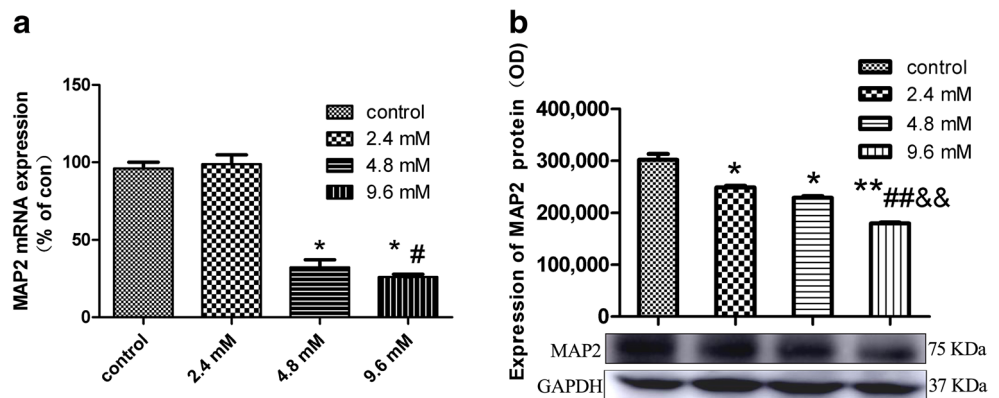
in organs, such as the liver, kidneys, lungs, brain, spleen, heart, muscles and bones (ATSDR US 2007). Various male and female animals were used for investigation of lead poisoning; chronic lead exposure altered DNA methylation in male Wistar rats (Sun et al. 2017) and impaired vesicle dynamics and release in the hippocampus of females (Guariglia et al. 2016). However, no significant differences were observed between female and male pups in a previous study (Gąssowska et al. 2016). Therefore, we used Kunming mice regardless of gender in our study.

Lead can cross the blood-brain barrier and enter the body of animals, affecting respiration, digestion, immunity and skeletal, reproductive, nervous and cardiovascular systems, leading to growth and development abnormalities in animals (Gillis et al. 2012). Overwhelming evidence proves the neurotoxicity of Pb and its detrimental effects on neurons. Lead poisoning mainly causes brain and neurological defects, including cognitive disorders, coordination impairment, hearing and visual disturbances (Leasure et al. 2008). In our study, lead acetate was orally administered to Kunming mice, and histopathological results showed the disordered molecular layer of the brain in the high-dose groups and the significantly decreased number of granular and pyramidal cells, especially in the 9.6-mM group. Ultrastructural changes were observed in brain tissues; these changes include distortion and swelling of the mitochondria, aggregation of chromatin, incomplete nuclear membranes, fractured and lost mitochondria cristae and reduced number of microtubules. These results offer a histopathological explanation for the cerebral cortex damage in Pb-exposed mice.

Dai et al. (2017) suggested that elevated Pb levels can result in adverse changes in blood morphology, haemoglobin synthesis and CR1 expression, which may be a non-negligible threat to the development of erythrocyte immunity in local preschool children. In the present study, lead accumulation in the blood was tested by AAS. Compared with the controls, a notable increase in lead concentration was observed in the blood of mice from the treatment groups ($P < 0.01$). TEM-EDS is based on X-ray quantum spectral curve and can be used for qualitative and quantitative analyses of samples at a general point, in a line or in surface analysis (Verma et al. 2017). In this experiment, lead was not detected in the brains of mice in the 2.4-mM group, and this result was probably due to the small amounts of Pb that were removed from the body during metabolism or lower intracellular Pb levels in comparison with the detection limits of the spectrometer resolution. Pb^{2+} was detected in nuclear pores, chromatin and nuclear membranes of mouse brain nerve cells in the 4.8- and 9.6-mM groups. Pb^{2+} was mainly located in the nuclear envelope in the brain cells of mice from the 4.8-mM group, whereas it was mainly found in the nuclear pores in the 9.6-mM group.

Lead exposure significantly decreases spine density and down-regulates the expression of NR2B subtype of N-methyl D-aspartate (NMDA) receptors, thereby inducing deficits in long-term potentiation and spatial learning processes (Nihei and Guilarte 2001; Neal et al. 2011; Yang et al. 2016). Lead exposure also altered presynaptic vesicle distribution in these hippocampal regions (Guariglia et al. 2016). MAP2 plays a role in neuronal polarity and neuronal dendritic growth, possibly by increasing the growth and repair rate of

Fig. 5 The effect of lead on MAP2 mRNA and protein expression levels. **a** mRNA expression, **b** protein expression. Control represents untreated mice. *Significantly different from the control ($P < 0.05$). #Significantly different from the 2.4 mM group ($P < 0.05$)



microtubules (Dehmelt and Halpain 2004). Our study revealed that high doses Pb reduced MAP2 mRNA and protein expression, especially in the 4.8- and 9.6-mM treatment groups ($P < 0.05$). The toxic effects were manifested in a dose-dependent manner and showed no influence on transcription in the low-concentration group (2.4 mM, $P > 0.05$). On the basis of these results, we speculate that Pb exerts direct toxic effects on neurons, destroying microtubules that cannot be repaired over time and limits functional abilities of the brain.

Conclusion

Observations on histopathological and morphological features of cells suggest that different lead concentrations exert direct toxic effects on neuronal cells of the brain. Lead not only circulated in the blood but also accumulated in nuclear pores, chromatin and nuclear membranes of mouse brain nerve cells. Expression levels of MAP2 mRNA and protein reduced in the treatment groups with increasing lead dosage. These results suggest that high lead levels enhance instability of microtubules in mouse brain tissues, affecting cytoskeleton assembly and mitosis, further damaging brain development and function. Results of this study provide a theoretical basis for further investigation of the mechanism of lead poisoning.

Funding This work was supported by the National Science Foundation of China (No. U1404329), Postdoctoral Science Foundation of China (No. 2014M561205), Scientific and Technological Foundation of Henan Province in China (172102110026) and Scientific and Technological Foundation of Henan Province Department of Education in China (No. 14A230006).

References

- Anjum MR, Madhu P, Reddy KP, et al (2016) The protective effects of zinc in lead-induced testicular and epididymal toxicity in Wistar rats. *Toxicol Ind Health*, 0748233716637543
- ATSDR, U. S (2007) Toxicological profile for lead. US Department of Health and Human Services, 1: 582
- Bansod B, Kumar T, Thakur R et al (2017) A review on various electrochemical techniques for heavy metal ions detection with different sensing platforms. *Biosens Bioelectron* 94:443–455. <https://doi.org/10.1016/j.bios.2017.03.031>
- Caldas D, Pestana IA, Almeida MG, Henry FC, Salomão MSMB, de Souza CMM (2016) Risk of ingesting As, Cd, and Pb in animal products in north Rio de Janeiro state, Brazil. *Chemosphere* 164: 508–515. <https://doi.org/10.1016/j.chemosphere.2016.08.130>
- Chen J, Kanai Y, Cowan NJ, Hirokawa N (1992) Projection domains of MAP2 and tau determine spacings between microtubules in dendrites and axons. *Nature* 360(6405):674–677. <https://doi.org/10.1038/360674a0>
- Chen L, Chen H, Yao C, Chang C, Xia H, Zhang C, Zhou Y, Yao Q, Chen K (2015) The toxicity of NaF on BmN cells and a comparative proteomics approach to identify protein expression changes in cells under NaF-stress: impact of NaF on BmN cells. *J Hazard Mater* 286: 624–631. <https://doi.org/10.1016/j.jhazmat.2014.12.056>
- Dai Y, Huo X, Zhang Y, Yang T, Li M, Xu X (2017) Elevated lead levels and changes in blood morphology and erythrocyte CR1 in preschool children from an e-waste area. *Sci Total Environ* 592:51–59. <https://doi.org/10.1016/j.scitotenv.2017.03.080>
- de Oliveira TM, Peres JA, Felsner ML et al (2017) Direct determination of Pb in raw milk by graphite furnace atomic absorption spectrometry (GF AAS) with electrothermal atomization sampling from slurries. *Food Chem* 229:721–725. <https://doi.org/10.1016/j.foodchem.2017.02.143>
- Dehmelt L, Halpain S (2004) The MAP2/Tau family of microtubule-associated proteins. *Genome Biol* 6(1):204. <https://doi.org/10.1186/gb-2004-6-1-204>
- Farzin L, Amiri M, Shams H, Ahmadi Faghih MA, Moassesi ME (2008) Blood levels of lead, cadmium, and mercury in residents of Tehran. *Biol Trace Elem Res* 123(1):14–26. <https://doi.org/10.1007/s12011-008-8106-y>
- Flora G, Gupta D, Tiwari A (2012) Toxicity of lead: a review with recent updates. *Interdiscip Toxicol* 5(2):47–58. <https://doi.org/10.2478/v10102-012-0009-2>
- Gąssowska M, Baranowska-Bosiacka I, Moczyłowska J et al (2016) Perinatal exposure to lead (Pb) promotes Tau phosphorylation in the rat brain in a GSK-3 β and CDK5 dependent manner: relevance to neurological disorders. *Toxicology* 347:17–28
- Gillis BS, Arbieva Z, Gavin IM (2012) Analysis of lead toxicity in human cells. *BMC Genomics* 13(1):344. <https://doi.org/10.1186/1471-2164-13-344>
- Guariglia SR, Stansfield KH, McGlothlin J, Guilarte TR (2016) Chronic early life lead (Pb²⁺) exposure alters presynaptic vesicle pools in hippocampal synapses. *BMC Pharmacol Toxicol* 17(1):56. <https://doi.org/10.1186/s40360-016-0098-1>
- Gulson B, Mizon K, Korsch M, Taylor A (2016) Revisiting mobilisation of skeletal lead during pregnancy based on monthly sampling and cord/maternal blood lead relationships confirm placental transfer of lead. *Arch Toxicol* 90(4):805–816. <https://doi.org/10.1007/s00204-015-1515-8>
- Gumy LF, Katrukha EA, Grigoriev I, Jaarsma D, Kapitein LC, Akhmanova A, Hoogenraad CC (2017) Map2 defines a pre-axonal filtering zone to regulate kif1- versus kif5-dependent cargo transport in sensory neurons. *Neuron* 94(2):347–362. <https://doi.org/10.1016/j.neuron.2017.03.046>
- Jannuzzi AT, Alpertunga B (2016) Evaluation of DNA damage and DNA repair capacity in occupationally lead-exposed workers. *Toxicol Ind Health* 32(11):1859–1865. <https://doi.org/10.1177/0748233715590919>
- Jin X, Xu Z, Zhao X, Chen M, Xu S (2017) The antagonistic effect of selenium on lead-induced apoptosis via mitochondrial dynamics pathway in the chicken kidney. *Chemosphere* 180:259–266. <https://doi.org/10.1016/j.chemosphere.2017.03.130>
- Kazemeini F, Malayeri BE, Chehregani A et al (2013) Identification of the heavy metals accumulator plants in surrounding area of mine. *Int J Agric Crop Sci* 6(10):565
- Kubatiev AA, Pal'tsyn AA (2012) Intracellular brain regeneration: a new view. *Vestnik Rossiiskoi akademii meditsinskikh nauk* 8:21–25
- Leasure JL, Giddabasappa A, Chaney S, Johnson JE Jr, Pothakos K, Lau YS, Fox DA (2008) Low-level human equivalent gestational lead exposure produces sex-specific motor and coordination abnormalities and late-onset obesity in year-old mice. *Environ Health Perspect* 116(3):355–361. <https://doi.org/10.1289/ehp.10862>
- Nascimento CRB, Risso WE, dos Reis Martinez CB (2016) Lead accumulation and metallothionein content in female rats of different ages and generations after daily intake of Pb-contaminated food. *Environ Toxicol Pharmacol* 48:272–277. <https://doi.org/10.1016/j.etap.2016.11.001>
- Neal AP, Worley PF, Guilarte TR (2011) Lead exposure during synaptogenesis alters NMDA receptor targeting via NMDA receptor inhibition. *Neurotoxicology* 32(2):281–289

- Nihei MK, Guilarte TR (2001) Molecular changes in glutamatergic synapses induced by Pb²⁺: association with deficits of LTP and spatial learning. *Neurotoxicology* 22(5):635–643. [https://doi.org/10.1016/S0161-813X\(01\)00035-3](https://doi.org/10.1016/S0161-813X(01)00035-3)
- Piechnik CA, Höckner M, de Souza MRDP, Donatti L, Tomanek L (2017) Time course of lead induced proteomic changes in gill of the Antarctic limpet *Nacella Concinna* (Gastropoda: Patellidae). *J Proteome* 151:145–161. <https://doi.org/10.1016/j.jprot.2016.04.036>
- Rosen MB, Pokhrel LR, Weir MH (2017) A discussion about public health, lead and *Legionella pneumophila* in drinking water supplies in the United States. *Sci Total Environ* 590:843–852
- Shenai-Tirodkar PS, Gauns MU, Mujawar MWA, Ansari ZA (2017) Antioxidant responses in gills and digestive gland of oyster *Crassostrea madrasensis* (Preston) under lead exposure. *Ecotoxicol Environ Saf* 142:87–94. <https://doi.org/10.1016/j.ecoenv.2017.03.056>
- Sohail M, Khan MN, Qureshi NA, Chaudhry AS (2017) Monitoring DNA damage in gills of freshwater mussels (*Anodonta anatina*) exposed to heavy metals. *Pak J Zool* 49(1):305–311. <https://doi.org/10.17582/journal.pjz/2017.49.1.305.311>
- Sun H, Wang N, Nie X, Zhao L, Li Q, Cang Z, Chen C, Lu M, Cheng J, Zhai H, Xia F, Ye L, Lu Y (2017) Lead exposure induces weight gain in adult rats, accompanied by DNA hypermethylation. *PLoS One* 12(1):e0169958. <https://doi.org/10.1371/journal.pone.0169958>
- Suzuki N, Ando S, Sumida K, Horie N, Saito K (2011) Analysis of altered gene expression specific to embryotoxic chemical treatment during embryonic stem cell differentiation into myocardial and neural cells. *J Toxicol Sci* 36(5):569–585. <https://doi.org/10.2131/jts.36.569>
- Verma M, Tyagi I, Chandra R, Gupta VK (2017) Adsorptive removal of Pb (II) ions from aqueous solution using CuO nanoparticles synthesized by sputtering method. *J Mol Liq* 225:936–944. <https://doi.org/10.1016/j.molliq.2016.04.045>
- Verstraeten SV, Aimo L, Oteiza PI (2008) Aluminium and lead: molecular mechanisms of brain toxicity. *Arch Toxicol* 82(11):789–802. <https://doi.org/10.1007/s00204-008-0345-3>
- Wagner PJ, Park HR, Wang Z, Kirchner R, Wei Y, Su L, Stanfield K, Guilarte TR, Wright RO, Christiani DC, Lu Q (2017) In vitro effects of lead on gene expression in neural stem cells and associations between up-regulated genes and cognitive scores in children. *Environ Health Perspect* 125(4):721–729. <https://doi.org/10.1289/EHP265>
- Yang QQ, Xue WZ, Zou RX, Xu Y, Du Y, Wang S, Xu L, Chen YZ, Wang HL, Chen XT (2016) β -Asarone rescues Pb-induced impairments of spatial memory and synaptogenesis in rats. *PLoS One* 11(12):e0167401. <https://doi.org/10.1371/journal.pone.0167401>
- Zhang YW, Yan L, Huang L (2016) Cerebral ganglion ultrastructure and differential proteins revealed using proteomics in the aplousiid (*Notarcus leachii cirrosus* Stimpson) under cadmium and lead stress. *Environ Toxicol Pharmacol* 46:17–26. <https://doi.org/10.1016/j.etap.2016.06.021>